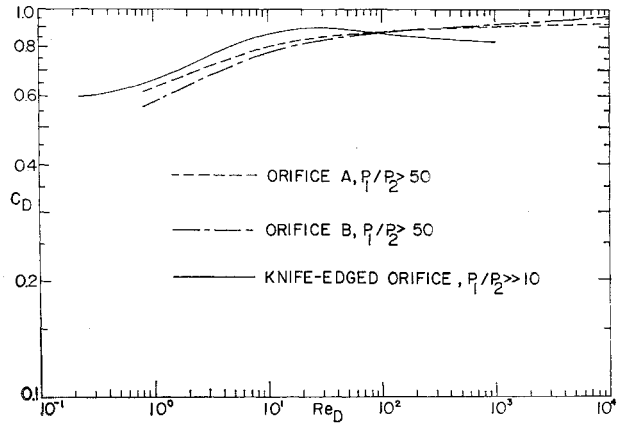

Fig. 2 Orifice results.

closely approximated by using the arc length of the entrance rather than the straight length from the entrance plane. In the case of Carley and Smetana's experiment this would give a total effective length of 7.32 cm and an L/D of 6.37. This effective length should probably be even greater due to the larger surface area seen by the flow in the smooth entrance, which is not fully accounted for by using the arc length alone. Hence, in this region, it is also not accurate to attempt comparison with a theory accounting for only the tube length downstream of the entrance even though this does make the assumption of fully developed flow at the effective entrance more valid.

One of the main reasons, the rounded entrance is used in experiments is to prevent entrance flow separation at larger Reynolds numbers and thus allow more favorable comparison with theories which do not account for separation. It is noted, however, in Fig. 1 that at the highest Reynolds numbers at which data were taken for the square-edged tube there is no indication of entrance separation. One would expect such separation to reduce the discharge coefficient significantly, causing a lower flow rate in the tube with the abrupt entrance than for the smooth entrance case. The opposite is indicated in the figure. However, this trend should change as the Reynolds number continues to increase and inertial effects assume increasing importance. Increased inertial effects should cause entrance separation and the vena-contracta effect reducing the discharge coefficient in the tube with the square-edged entrance. It appears that if the data were extended to higher values of Reynolds number a maximum would be reached for the discharge coefficient through the square-edged tube beyond which there would be a decrease and a crossing of the two curves.

This analysis is supported by the earlier orifice data of Smetana, Sherrill, and Schort[5] as shown in Fig. 2. Orifice A had an entry radius of 0.317 cm with a 1.15-cm diam opening. Orifice B had the same opening diameter with a 0.579 cm entry radius. The comparison with a thin knife edge orifice exhibits the maximum in discharge coefficient which preceeds a decrease to a limit somewhat below that for the other 2 orifices.

Conclusions and Recommendations

The bell-mouth entry which is used by most experimentors in tube flow study may give deceptive results for flows at low Reynolds numbers. At free molecule conditions, the effective length of the tube is shorter than the actual tube length but not as short as it would be if the entrance length is neglected. In the upper transition or slip-flow regime, the effective tube length is longer than the distance between the entrance and exit planes and results in deceptively low discharge coefficients. It is only above the Reynolds number for entrance separation that the smooth entrance tube provides a better comparison with tube flow theory.

Unfortunately, it is not yet possible to predict the occurrence of entrance separation accurately for tubes of varying lengths. It has long been suggested that the onset of separation is a function of L/D and $L/(DRe_D)$. However, neither theory nor experiment has yet determined this relationship. Hence, the experimentor should carefully choose his entrance shape when working with low Reynolds number flows, choosing the square-edged entrance in the transition to free-molecule range and the smooth entrance in the slip to continuum region. Proper entry choice should result in more meaningful comparison between experiment and existing theory.

References

[1] Carley, C. T., Jr. and Smetana, F. O., "Experiments on Transition Regime Flow through a Short Tube with a Bellmouth Entry," *AIAA Journal*, Vol. 4, No. 1, Jan. 1966, pp. 47–54.

[2] Clausing, P., "Über die Stromung sehr verdunnter Gase durch Rohren von beliebiger Lange," *Annalen der Physik*, Vol. 12, No. 8, March 1932, pp. 961–989.

[3] Knudsen, M. H. C., *The Kinetic Theory of Gases*, Methuen, London, 1934.

[4] Marchman, J. F., III, "The Effect of Length-to-Diameter Ratio on Flow through a Short Tube with a Square-Edged Entrance in the Transition Flow Regime," Ph.D. Thesis, North Carolina State University, Raleigh, N. C., 1968.

[5] Smetana, F. O., Sherrill, W. A., and Schort, D. A., Jr., "Measurements of the Discharge Characteristics of Sharp-Edged and Round-Edged Orifices in the Transition Regime," *Rarefied Gas Dynamics*, Vol. 2, Academic Press, New York, 1967, pp. 1243–1256.

[6] Sreekanth, A. K., "An Experimental Investigation of Mass Flow through Short Circular Tubes in the Transition Flow Regime," Rept. D1-0427, April 1965, Boeing Scientific Research Labs., Seattle, Wash.

A Study of High-Velocity (4.0–6.5 cm/μ sec) Jet Propagation through Expansion Chambers

H. David Glenn* and Barbara K. Crowley†
Lawrence Radiation Laboratory, University of California, Livermore, Calif.

Introduction

In recent years, considerable effort has been expended in studying the propagation of high-energy gas jets. One aspect of this work has been the development of experimental[1–3] techniques for investigating the radiation precursor associated with the propagation of high-velocity gas jets under low-pressure conditions. These experiments have encouraged qualitative discussions[4–6] and theoretical models[3,7] for interpreting and understanding the precursor phenomenon.

The present report describes two Voitenko[8] compressor experiments which were conducted to study the radiation precursor and the effects of divergence and expansion chambers on the propagation of plasma gas jets. In the first experiment, the compressor was connected to a steel outlet pipe, as shown in Fig. 1. In the second experiment, a constant 2.7 cm diam was maintained across the two expansion sections. By direct comparison of the experimental TOA (time-of-arrival) results, the relative effect of chambers on high-velocity gas

Received January 30, 1969; revision received June 16, 1969. Work performed under the auspices of the U.S. Atomic Energy Commission.

* Research Physicist.
† Physicist. Member AIAA.

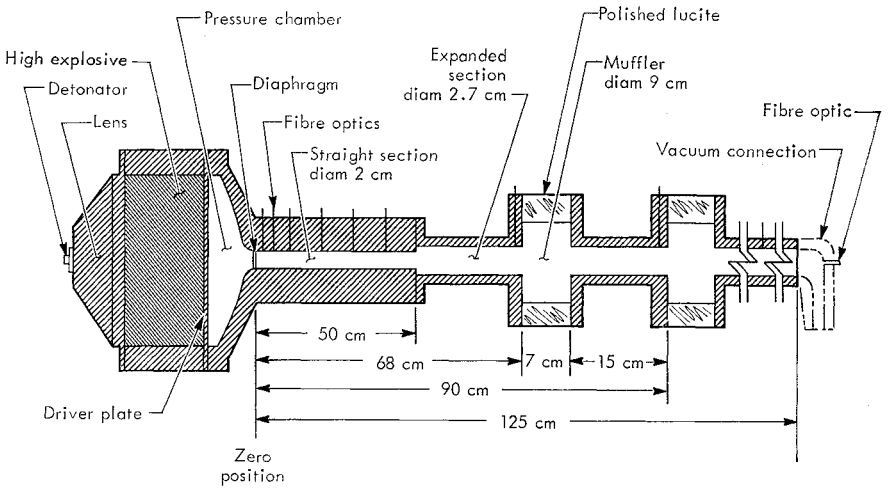

Fig. 1 Compressor assembly, outlet pipe, and diagnostics systems used in plasma jet propagation studies.

jets was examined. In addition, certain characteristics (e.g., radial and axial shape, luminosity profile) of the gas jet were identified.

Experimental System

The principal features of the compressor and outlet pipe are illustrated in Fig. 1. The high explosive drives a metallic plate that compresses the chamber air (pressure initially at 11.2 bars) into a small volume and high pressure before the 0.025-cm-thick aluminized‡ Mylar diaphragm breaks. This highly compressed plasma gas then jets down a smooth (40-μ-cm honed finish[9]) 2-cm-i.d. steel outlet pipe. The two experiments were conducted with an initial pressure of 25 μ in the outlet pipes.

As the plasma jet moved down the outlet pipe, its TOA and luminosity were monitored[10] by light pipes[11,12] (fiber optics) placed at preselected positions in the steel pipe. One end of each light pipe was recessed 0.32 cm from the inner wall of the outlet pipe and viewed the bore through a 0.16-cm circular hole in the steel wall. The light pipes were then brought radially out through the steel wall and tied into a display board. In addition, a light pipe was mounted in the vacuum connected (Fig. 1) and was oriented to look axially up the outlet pipe. This light pipe was used to determine the time at which the jet emerged from the diaphragm. As the plasma jet progressed down the outlet pipe, luminosity was transmitted via the light pipes to the external board which was scanned by a streaking camera. The writing speed of the streaking camera for both experiments was 5.0 cm/μsec.

In the first experiment, the side walls of the expansion chambers were fitted with polished lucite windows. Framing

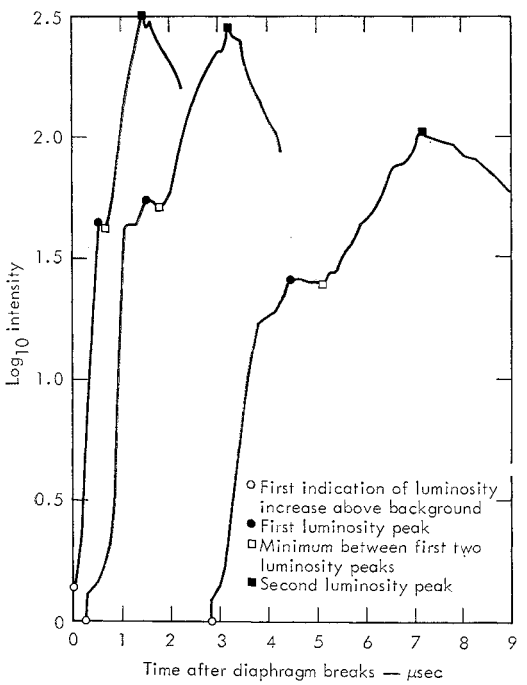

Fig. 2 Luminosity profiles of jet plasma propagation for light pipes at 4.77, 9.78, and 29.79 cm from the diaphragm.

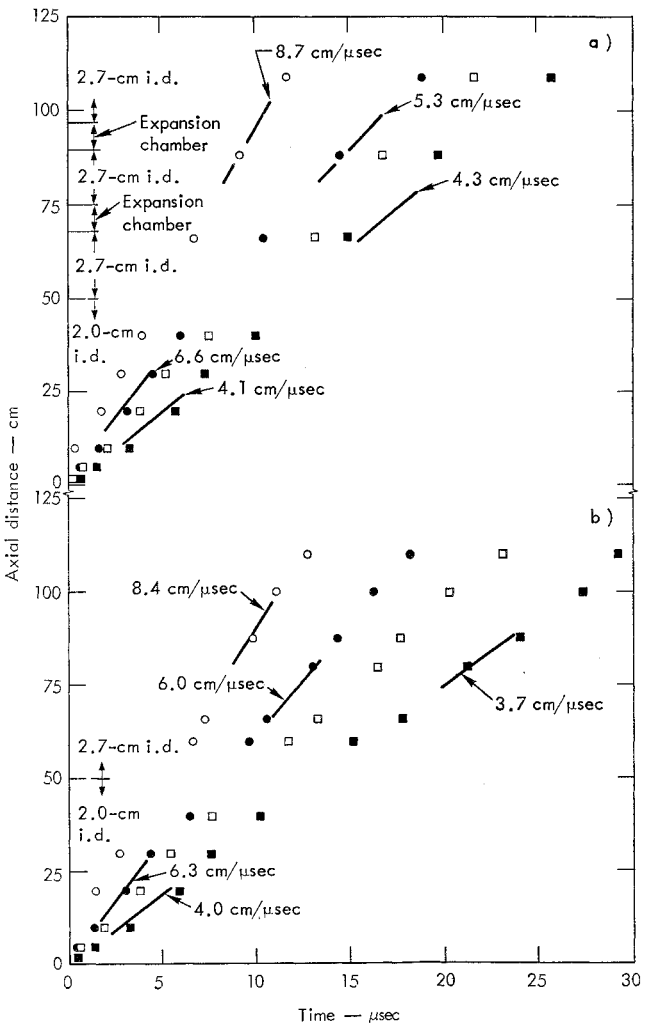

Fig. 3 a) Plasma jet motion for the experiment with expansion chambers and b) plasma jet motions for the experiment without expansion chambers.

‡ Aluminized to reflect the luminosity until the diaphragm breaks.

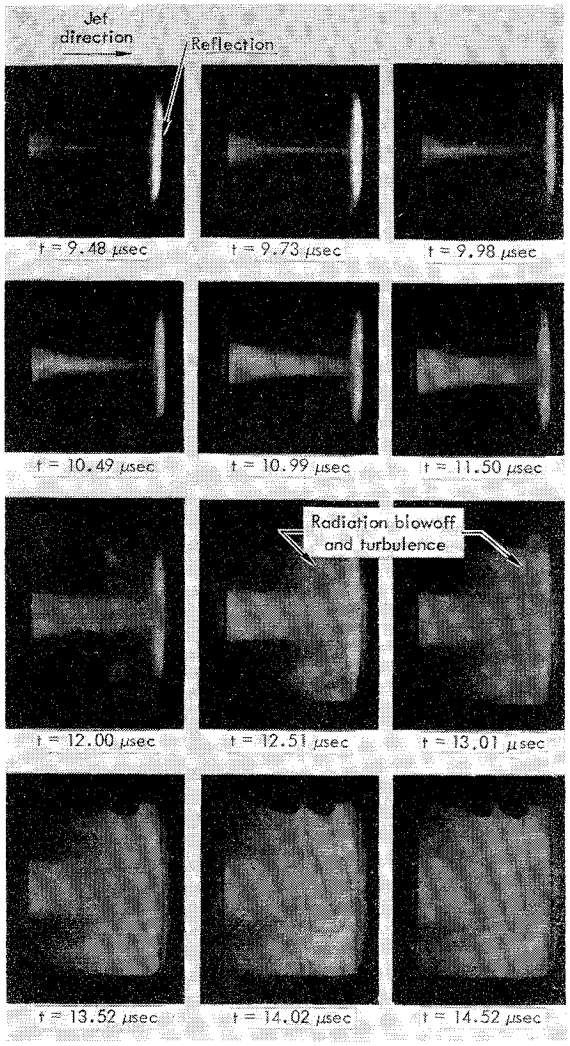

Fig. 4 Passage of jet plasma through the first expansion chamber at various times after the diaphragm breaks.

cameras focused on the windows recorded the radial and axial progress of the jet as it moved through the chambers. These motion picture studies provide a more qualitative understanding of the interaction of the jet with the chambers.

Experimental Results and Discussion

A Wratten 57 optical filter was used on the streaking cameras which monitored the light pipes. This filter reduced exposure to a linear region of the film response curve. This curve was determined by using a photographic step tablet and Xenon flash tube. The curve was used to convert the densitometer readings of the light pipe traces into the jet plasma luminosity profiles shown in Fig. 2 for the light pipes at 4.77, 9.78, and 29.79 cm from the downstream center of the Mylar diaphragm. These profiles are representative of light pipe luminosity outputs all along the outlet pipe.

To characterize the plasma jet motion down the outlet pipe, four TOA points (see Fig. 2) from each light pipe record are plotted in Figs. 3a and 3b. The TOA plots indicate that a gradual dispersion of the luminosity peaks is taking place as the plasma jet continues down the outlet pipe.

The first indication of luminosity is observed simultaneously with the diaphragm breaking time (within an experimental error of 0.06 μsec) at the first two light pipes located at 2 and 5 cm. Therefore, this first luminosity point appears to be a radiation precursor phenomenon.

The first, relatively low, luminosity peak is the second point plotted; it has a velocity ≈6 cm/μsec. If the density of this 6-cm/μsec portion of the jet was comparable to the density of atmospheric air (10^{-3} g/cm^3), it would act like a 6-cm/μsec piston, and a shock with velocity >6 cm/μsec would be generated in atmospheric air. However, when atmospheric air was used in an outlet pipe, a shock with velocity 4 cm/μsec was generated.[13] Consequently, the 6 cm/μsec portion of the jet is probably a relatively low density ($<10^{-3}$ g/cm^3).

The second luminosity peak travels at about 4 cm/μsec and has a much greater intensity than the first peak. The chamber gas jet that generated the 4-cm/μsec air shock was calculationally shown to have a velocity of nearly 4 cm/μsec and densities in excess of 10^{-2} g/cm^3.[13] Because of the similar velocities and much larger luminosities, the second peak may be associated with this higher-density section of the jet.

A significant feature of Fig. 3 is that there appears to be little velocity attenuation of the first two luminosity peaks. Therefore, the propagation of those regions of the plasma jet which are associated with the peaks appear to be little affected by interactions (such as friction, heat transfer, ablation) with the pipe walls. By contrast, a similar experiment that was performed with a straight, 2-cm-i.d. outlet pipe containing atmospheric air indicated an attenuation of the air shock velocity from 4 to about 1.6 cm/μsec within 70 diameters. Theoretical studies[13] attributed this attenuation to wall interactions in the high-energy and high-density shocked air region. By comparing Figs. 3a and 3b, it also appears that the expansion chambers had little effect on the propagation of the regions of the plasma jet which are associated with the luminosity peaks.

Motion of the plasma jet through the two expansion chambers of the first experiment was recorded by a framing camera with optical filters. To determine just what optical filters would be needed, a preliminary experiment with similar expansion chambers was performed. A Beckman and Whitley 189B with a ND 2.0 filter was focused on the first chamber. A second framing camera (LRL Model 6) with a ND 1.0 filter was focused on the second expansion chamber. High-speed Ektachrome film was used in both cameras. Figure 4 shows passage of the jet plasma through the first chamber at various times. Results for the second chamber were similar to those shown in Fig. 4, but not as well defined because of slight overexposure. Comparison of the photographic results at various times with Fig. 3a indicates the first peak underwent little radial expansion in passage through the chambers. Radiation blowoff from the chamber wall and turbulence tended to obscure photographs at a time just prior to arrival of the second peak.

References

[1] Weyman, H. D., "Electron Diffusion Ahead of Shock Waves in Argon," *The Physics of Fluids*, Vol. 3, No. 4, 1960, pp. 545–548.

[2] Lubin, M. J. and Resler, E. L., Jr., "Precursor Studies in an Electromagnetic Driven Shock Tube," *The Physics of Fluids*, Vol. 10, No. 1, 1967, pp. 1–8.

[3] Holmes, L. B., "Plasma Density Ahead of Pressure Driven Shock Waves," Rept. AFOSR 65-0974, 1965, University of Rochester.

[4] Zel'dovich, Y. B. and Raizer, Y. P., *Physics of Shock Waves and High Temperature Hydrodynamic Phenomena*, Academic Press, New York, 1966, Chapt. IX.

[5] Gross, R. A., "Strong Ionizing Shock Waves," *Reviews of Modern Physics*, Vol. 37, No. 4, 1965, pp. 724–743.

[6] Zinman, W. G., "Comment on Experimental Precursor Studies," *AIAA Journal*, Vol. 4, No. 11, Nov. 1966, pp. 2073–2075; also Weymann, H. D., "Comments on Precursors Ahead of Pressure Driven Shock Waves," *AIAA Journal*, Vol. 5, No. 7, July 1967, pp. 1375–1376.

[7] Wilson, D. S. and Lin, T. C., "Impurity Photoionization Theory of Precursors," PIBAL Rept. 1006, 1967, Polytechnic Institute of Brooklyn.

[8] Voitenko, A. E., "Generation of High-Speed Gas Jets," *Soviet Physics Doklady*, Vol. 9, No. 10, 1966, pp. 860–862; also "Strong Shock Waves in Air," *Soviet Physics-Technical Physics*, Vol. 11, No. 1, 1966, pp. 128–130.

[9] *Surface Texture*, American Standard ASA B46.1, 1962, The American Society of Mechanical Engineers, New York.

[10] Glenn, H. D. and Crowley, B. K., "Optical Technique for Monitoring High Energy Shocks in Steel Pipes Containing Ambient Atmospheric Air," Rept. UCRL-71007, 1968, Lawrence Radiation Lab., Livermore.

[11] Kapany, N. S., *Fiber Optics*, Academic Press, New York, 1967.

[12] Goettelman, R. C. and Crosby, J. K., "Optical Probe Techniques," *The Review of Scientific Instruments*, Vol. 35, No. 11, 1964, pp. 1546–1549.

[13] Crowley, B. K. and Glenn, H. D., "Numerical Simulation of a High Energy (Mach 120 to 40) Air Shock Experiment," presented at the Seventh International Shock Tube Symposium, Toronto, Canada, June 1969.

Supersonic Wake Flow Visualization

THOMAS J. MUELLER,* CHARLES R. HALL JR.,† AND WAYNE P. SULE‡
University of Notre Dame, Notre Dame, Ind.

Introduction

THERE has been great interest throughout the history of aerodynamics in making flow patterns visible. In addition to the qualitative picture of the flow hoped for, the possibility of obtaining quantitative flow measurements without introducing probes which invariably disturb the flow has provided the necessary incentive for development of these techniques. Optical methods of investigation which depend on density changes are especially suited to the visual study of supersonic flows. The interferometer, the schlieren, and the shadowgraph are commonly used optical methods of this type.

The use of smoke for flow visualization at low subsonic speeds is quite common and may be traced to L. Mach of Vienna in 1893.[1] Mach used an indraft low-speed wind tunnel (10 m/sec) with a piece of wire mesh to straighten the flow. The flow was observed and photographed by using silk threads, cigarette smoke, and glowing iron particles. The production of well-defined smoke streamlines (i.e., steady-state streaklines) at supersonic speeds was first accomplished by V. P. Goddard at the University of Notre Dame in 1959.[2] V. P. Goddard also developed a modified schlieren system that permits the simultaneous photographing of both the smoke and shock wave patterns. When nitrous oxide is used in place of smoke, the streamlines become visible along with the shock pattern in any ordinary schlieren system. The principal objectives of the investigation described herein were to extend and to improve supersonic flow visualization techniques for the study of laminar supersonic wake flows.

Experimental Apparatus and Technique

A schematic diagram of the small indraft planar supersonic smoke tunnel (PSST) utilized for these experiments is shown in Fig. 1. The PSST consists of inlet screens, contraction section, nozzle section including a plug which produces a wake, and a diffuser section. A total of seven inlet screens are located at the inlet to the contraction section in order to reduce the turbulence level of the flow. The contraction section has about a 100:1 contraction in area to the nozzle throat without the plug. With the plug in position, the contraction in area is about 200:1. The nozzle section consists of a contoured planar nozzle with a $\frac{1}{2}$-in. piece of lucite in the center of the nozzle block. The parallel outflow nozzle was designed for a Mach number of 1.40 and had a 2.5-in.[2] test section. A lucite wedge-shaped plug with a rounded leading edge was inserted into the nozzle to produce a wake. This configuration resembles a plug nozzle referred to as the expansion-deflection nozzle, or may be thought of as representing a strut, a flame holder, a scram-jet fuel injector, etc. The diffuser section connects the nozzle with a continuous operation vacuum pump that produces a pressure difference of 18 in. of mercury. A somewhat larger, though geometrically similar, PSST with a planar expansion-deflection nozzle test section was also used in this investigation. This larger nozzle section (i.e., about 4 in. × 5 in. in the working section downstream of the plug) contained an adjustable total and/or static pressure probe for conventional measurements. A complete description of this PSST is given in Ref. 3. Auxiliary equipment includes smoke generator and smoke rake, schlieren systems (to be described below), pressure taps, probes and manometers, high intensity lights, and a camera.

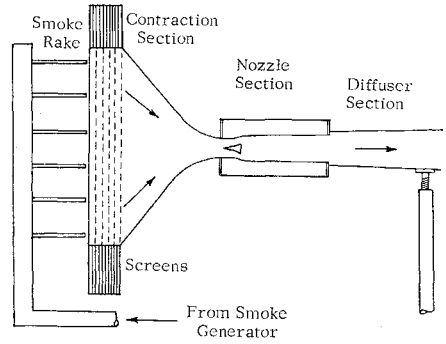

Fig. 1 Sketch of planar supersonic smoke tunnel.

A standard single-pass, parallel-light schlieren system was used. The standard schlieren system was converted to an opaque-stop system by replacing the slit source by a circular source and the knife edge by a small circular opaque-stop, i.e., a piece of glass with a $\frac{1}{16}$-in. diam spot. Proper adjustment of this system yields a schlieren picture where the undeflected light (i.e., no density gradient) hits the opaque stop producing a black background and deflected light misses the stop and shows up white. This black background is necessary for simultaneous schlieren and smoke photography. A single-frequency gas laser§ was also used as a light source in place of the 1000 w Bantam Super Spot in the opaque-stop schlieren system. Two double-convex lenses were used to diverge the laser beam for use in the schlieren system.

Smoke is generated by dripping kerosene on to electric strip heaters in each of the four legs of the generator. This smoke is forced to the smoke rake by a squirrel cage blower. By passing through a system of vertical pipes, the smoke is cooled to room temperature. Finally, the smoke passes through one or more of the horizontal tubes whose outlets are placed flush with the first screen at the PSST inlet. These tubes introduce the smoke into the PSST at any desired location.

Presented as Paper 69-346 at the AIAA 4th Aerodynamic Testing Conference, Cincinnati, Ohio, April 28–30, 1969; submitted April 23, 1969; revision received July 3, 1969. This research was jointly supported by the Department of Aerospace and Mechanical Engineering and NASA under Grant NsG(T)-65. The authors gratefully acknowledge the helpful comments of V. P. Goddard and A. A. Monkiewicz.

* Professor of Aerospace and Mechanical Engineering. Associate Fellow AIAA.

† NASA Fellow. Associate Member AIAA.

‡ Research Assistant. Associate Member AIAA.

§ Spectra-Physics Model 119, Helium-Neon Laser, wavelength 632.8 nanom, output power greater than 100 μw, uniphase, single frequency, beam divergence approximately 10 mrad.